Novel biaryl imines and amines as potential competitive inhibitors of dihydropteroate synthase

Warren Chang*[1], Vigasini Rajaram*[1], Harshith Yallampalli*[2], Arielle Dong[1], Kimberly Huang[1], Anirudh Valiveru[1], Edward Njoo[3]

[1] Mission San Jose High School, Fremont, California

[2] Irvington High School, Fremont, California

[3] Department of Chemistry, Biochemistry, & Physics, Aspiring Scholars Directed Research Program, Fremont, California

* Co-first Authors

SUMMARY

Antibiotic-resistant bacteria account for over 2.8 million infections and 35,000 deaths annually in the United States. The evolution of new resistant strains necessitates the continued development of new antimicrobial compounds. A target for further pharmaceutical development is the enzyme dihydropteroate synthase (DHPS), which plays a key role in prokaryotic biosynthesis of folic acid. A class of drugs called sulfonamides, including drugs sulfamethoxazole and sulfatrim, bind and act as competitive substrates to p-aminobenzoic acid (pABA), a substrate of DHPS, but are limited by their numerous side effects on the human body and bacterial resistance mutations that block larger molecules from entering the binding pocket. Here, we report the design, combinatorial synthesis, and antibacterial properties of a library of novel biaryl small molecules to target the binding pocket of DHPS. We hypothesize that the synthesized compounds in this study will have strong antibiotic efficacy because of their structural similarities to dihydropteroate, an intermediate in the biosynthesis of folate by the enzyme DHPS. Compounds were first screened in silico via docking to the binding pocket in DHPS. The antibiotic efficacy of these compounds was then tested on three species of bacteria related to human pathogens through a Kirby Bauer assay. Two hit compounds were discovered as having larger radii of inhibition compared to other compounds from the data of the assay. The larger radii of inhibition indicates that the bacteria tested against were susceptible to the use of the hit compounds. The results of the assay establish a definitive structure-activity relationship for the compounds studied and provide a basis for the future development of antibiotics targeting DHPS.

INTRODUCTION

Antibiotic resistance evolution is a rapidly growing problem in pharmaceutical development. In the United States alone, antibiotic-resistant bacterial or fungal infections cause more than 35,000 deaths annually (1). Due to the frequent use of a limited selection of commercial broad-spectrum antibiotics, mutations for antibiotic resistance are quite common and often render certain antibiotics ineffective (1).

As more antibiotics become clinically available, antibiotic-resistant strains of bacteria become stronger and increasingly resistant to available antibiotics. Antibiotic-resistant infections become progressively difficult or even impossible to treat (1). Additionally, many antibiotics can have negative side effects on the human body by damaging immune cells, causing allergic reactions, and killing healthy bacteria that protect the human body from fungal infections (2). For these reasons, the development of new small-molecule antibacterial agents is of great scientific and biomedical importance.

The enzyme dihydropteroate synthase (DHPS) is a common target for drug development. This is because it is a key enzyme in the prokaryotic biosynthesis of folic acid, a necessary cofactor in the nucleic acid biosynthesis pathways in almost all bacterial strains (3). DHPS facilitates the synthesis of 7,8-dihydropteroate via the coupling of p-aminobenzoic acid (pABA) and pterin, which bind to their respective binding pockets in the enzyme's active site. This enzyme has been an ideal target for antibiotics due to its necessity in bacterial systems and its absence in higher organisms, including humans (4).

Sulfonamides have been shown to possess antibiotic, antifungal, and anti-cancer properties. They are commonly used as a treatment for urinary tract infections (UTIs), bronchitis, eye infections, bacterial meningitis, pneumonia, ear infections, severe burns, and can act as anticancer agents (5-7). Many studies have shown that sulfonamide drugs are effective in competitively binding to the DHPS enzyme's pABA binding pocket, thereby inhibiting the folate biosynthetic route (5, 6). Recent studies have been conducted on the pterin binding pocket of DHPS, and molecules designed to inhibit this pocket have shown to be incredibly effective in inhibiting DHPS without the disadvantages of sulfonamide drugs, thus making it a promising new avenue for research (4, 8, 9). Unlike the pABA binding pocket, the pterin binding pocket is highly conserved due to the absence of flexible loop residues that are prevalent in the pABA binding pocket, which is predicted to cause fewer mutations against antibiotics (10). However, the application of these compounds is still in development due to poor solubility and absorption of pterin-based drugs.

In the process of developing new inhibitors for targets such as DHPS, many factors must be considered. For example, Lipinski's rule of five is a methodology that is useful in determining the drug-likeness of a molecule using five core rules and is used to develop small molecule inhibitors (11). In the process of developing small molecule inhibitors, combinatorial synthesis and structure-activity relationships are also prevalent. Combinatorial synthesis can be used to

screen a variety of similar molecules using various functional substitutions to identify potential hit molecules that can be further optimized to improve their efficacy. In the process of testing, a structure-activity relationship can also be derived from how well the molecules form and its interactions with the binding site. This provides baseline information that can be used to determine functional groups that increase binding affinity and the overall efficacy of the drug. The biaryl imine and amine compounds synthesized in this study were rationalized by their high structural similarity to the 7,8-dihydropteroate product of DHPS, and various functional groups were deemed appropriate from the hydrogen bonding interactions present in both the pterin and pABA binding pockets. This information is a good indicator of inhibition because the product of an enzyme is used for later processes in the case of the pABA and pterin binding pockets. The amine and imine compounds differ by one double bond, and this study aims to monitor the effects of the rigidity of these compounds and their effect on antimicrobial activity.

Through the combinatorial synthesis of biaryl imine and amine compounds with a variety of functional group substitutions to develop a structure-activity relationship of DHPS, this study aimed to identify compounds that inhibit DHPS. In this study, the synthesized compounds are hypothesized to demonstrate strong antibiotic efficacy due to their structural similarities to dihydropteroate, a crucial intermediate in the folate biosynthesis pathway facilitated by the enzyme DHPS. The antibiotics synthesized in this study resemble the dihydropteroate due to their biaryl structure. Therefore, the synthesized antibiotics are predicted to have an optimal structure for binding with the pterin-binding pocket of DHPS. The key binding elements of the pterin-binding pocket indicate that an antibiotic with structural similarities to dihydropteroate is most effective. As shown in Figure 1, dihydropteroate and the designed competitive inhibitor compounds have structural similarities.

The compounds in this study were screened against three species of bacteria: *S. epidermidis*, *E. coli,* and *B. cereus.* These species are closely related to many notable human pathogens, which allow for a more accurate determination of the applicability of these compounds in the medicinal field (12-14). Both *S. epidermidis* and *B. cereus* are gram-positive bacteria, while *E. coli* is gram-negative (12-14). Both gram-positive and gram-negative bacteria were used in this study to increase diversity in bacterial testing and to identify any differences in efficacy of the compounds between the two types of bacteria.

Two hit compounds were discovered to have a larger radius of inhibition compared to the other molecules synthesized. This was determined through a Kirby Bauer assay against the three bacteria strains used. This trend demonstrated that sulfanilic acid groups resulted in a higher radius if inhibition in
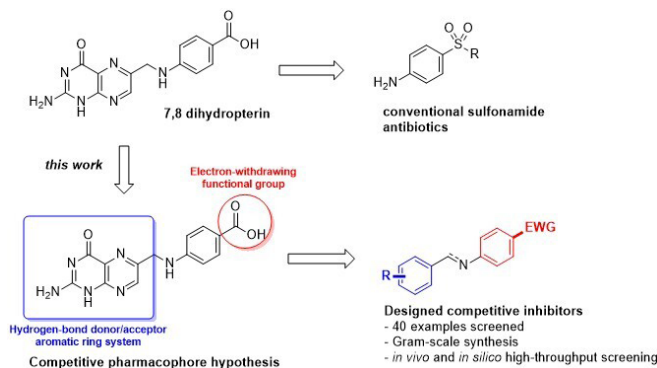

Figure 1: Structures of conventional sulfonamide antibiotics, dihydropteroate, and the designed competitive inhibitors used in this study. Both consist of a biaryl skeleton with various aryl substitutions, including an electron-withdrawing group on the para

comparison to the other molecules.

RESULTS
Synthesis results

Twenty imine compounds (**Table 1**; Compounds 2a-t**)** were combinatorially prepared by condensation of an aryl aldehyde 1 with an aniline 2 (**Figure 1**)**.** The twenty amine compounds (**Table 2**; Compounds 3a-t**)** were synthesized by borohydride reduction of the corresponding imine. We purified all compounds by recrystallization and characterized them by Fourier Transform Infrared (FT-IR) spectroscopy and liquid chromatography-mass spectrometry (LC-MS). Fourier Transform Infrared (FT-IR) spectroscopy and liquid chromatography-mass spectrometry (LC-MS) indicated that the compounds we created were synthesized correctly and were the molecules intended. A full reaction schematic can be seen in **Figure 2**.

Drug likeness screening results

In this study, we calculated the total polar surface area (TPSA), clogP, and drug likeness scores for all compounds using the Osiris Property Scanner. TPSA and clogP are both indicators of the polarity of the compound, which is necessary in determining the bioavailability of these compounds, due to solubility of small molecule inhibitors being a huge issue in antimicrobial drugs. The drug likeness score is an overall assessment of the molecule's likelihood of working well in the human body, and encompasses TPSA, clogP, molar mass, and functional groups that may be potentially cytotoxic to the human body (nitro NO_2^- groups being a primary example). Although most of these compounds did not exhibit great drug likeness scores, a noticeable trend was developed, in which amines demonstrated greater drug likeness scores compared to their respective imine compounds.
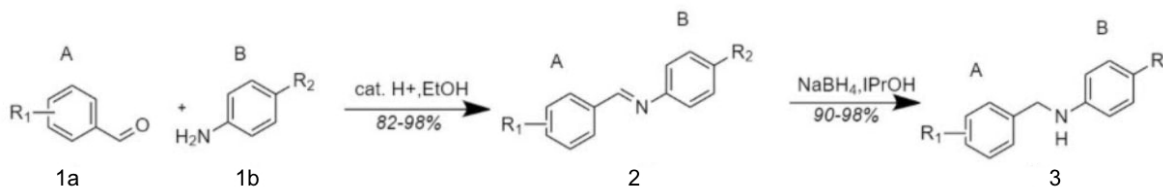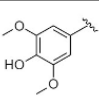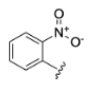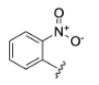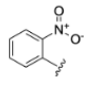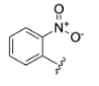

Figure 2: Reaction schematic with reagents and yields. The functional groups NO2, SO3H, SO2NH2, or COOH are present on the para position of the molecule. The possible R group substituents on the A ring can be seen in Table 1.

Table 1: Data on the imine compounds used in this study. Column 2 consists of diagrams of the R group substitution on the A ring for each imine compound. Column 3 shows the R2 groups for each imine compound. Column 4 shows TPSA (total polar surface area), values in angstroms. Column 5 has the cLogP value for each imine compound determining its partition coefficient between n-octanol and water. Column 6 shows the drug scores of each imine compound. Column 7 shows the docking scores calculated in kcal/mol.

Compound	Ring A	R₂	TPSA	cLogP	Drug Score	Docking Score
2a		COOH	79.12 Å²	2.51 nmoles/mg	0.44	-6.5 kcal/mol
2b		COOH	79.12 Å²	2.10 nmoles/mg	0.41	-6.5 kcal/mol
2c		COOH	52.9 Å²	2.41 nmoles/mg	0.27	-6.5 Kcal/mol
2d		COOH	52.9 Å²	2.03 nmoles/mg	0.56	-6.4 kcal/mol
2e		NO₂	87.64 Å²	2.10 nmoles/mg	0.42	-6.4 kcal/mol
2f		NO₂	87.64 Å²	1.70 nmoles/mg	0.35	-6.4 kcal/mol
2g		NO₂	61.42 Å²	2.01 nmoles/mg	0.25	-5.3 kcal/mol
2h		NO₂	96.87 Å²	1.63 nmoles/mg	0.43	-5.3 kcal/mol
2i		SO₃H	104.5 Å²	0.79 nmoles/mg	0.17	-6.6 kcal/mol
2j		SO₃H	104.5 Å²	0.39 nmoles/mg	0.15	-6.6 kcal/mol
2k		SO₃H	78.35 Å²	0.70 nmoles/mg	0.10	-5.6 kcal/mol
2l		SO₃H	113.8 Å²	0.32 nmoles/mg	0.21	-5.8 kcal/mol
2m		SO₂NH₂	110.3 Å²	1.79 nmoles/mg	0.50	-6.6 kcal/mol
2n		SO₂NH₂	110.3 Å²	1.38 nmoles/mg	0.61	-6.8 kcal/mol
2o		SO₂NH₂	84.14 Å²	1.69 nmoles/mg	0.36	-5.2 kcal/mol

Table 1 continued

2p		SO_2NH_2	119.5 Å^2	1.31 nmoles/mg	0.81	-5.7 kcal/mol
2q		COOH	95.48 Å^2	1.60 nmoles/mg	0.43	-6.0 kcal/mol
2r		NO_2	104.0 Å^2	1.19 nmoles/mg	0.41	-6.8 kcal/mol
2s		SO_3H	120.9 Å^2	-0.12 nmoles/mg	0.17	-6.1 kcal/mol
2t		SO_2NH_2	126.7 Å^2	0.88 nmoles/mg	0.43	-6.0 kcal/mol

Docking results

All 40 compounds were docked on *Yersinia pestis* DHPS (PDB:5JQ9), and docking scores were recorded (15). Predicted binding affinities by molecular docking are reported in the last column of **Tables 1 and 2**. Docked poses of select compounds along with hydrogen bonding interactions can be seen in **Figure 3**. All 40 compounds demonstrated higher binding affinity than the endogenous ligand, pterin, at 5.2 kcal/mol. The binding energy of the pterin substrate was used as a reference to demonstrate the greater affinity the enzyme had for the compounds in this study relative to pterin. Compounds **2n**, **2r**, **3m,** and **3n** were identified as hit compounds because they all had a docking score lower than or equal to -6.7. The low docking score indicates that the compounds bind well with the binding site in DHPS. This number was chosen because it indicated a statistically significant difference between the other compounds tested.

Kirby Bauer assay

The Kirby Bauer assay was used to determine the efficacy of our drugs (**Figure 4**). Agar plates containing our bacterial species were tested against all 40 compounds with concentrations of 10 mM and 1 mM. The Kirby Bauer assay was conducted on all imine and amine compounds as well as a negative control using three different bacterial species, *S. epidermidis*, *E. coli*, and *B. cereus*.
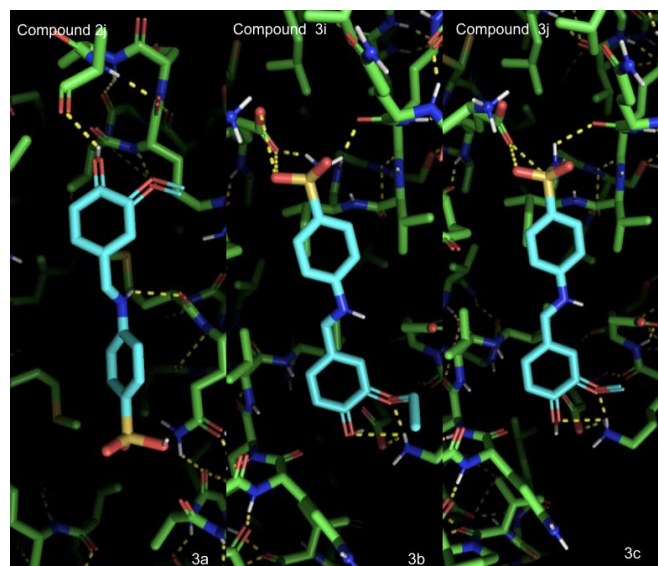
DISCUSSION

All 40 compounds were successfully synthesized and characterized via Infrared Spectroscopy. Both the imine synthesis and reductive amination are relatively simple reactions, with very few possible side products. Imine synthesis requires the presence of an electrophile on the aldehyde, resulting in a nucleophilic attack from the primary amine on the aniline. All the aldehydes used in this study have only one electrophilic carbon that is suitable for a nucleophilic substitution, which is located at the carbonyl site. Reductive amination requires the presence of a reducible group, which in this case is the imine functional group. The biaryl imine compounds synthesized from the previous step do not have any other reducible groups, so there are no possible side products of this reaction.

The FT-IR spectra were obtained and analyzed for respective imine and amine functional group shifts. Amine shifts were observed at 1600-1500 cm-1, which denotes an N-H shift, and at 1250-1335 cm-1 which denotes a C-N shift. Imine shifts were present at around 1690-1640 cm-1. One possibility for the compounds in this study is that the amines existed as protonated ammoniums due to the synthesis in an acidic environment. This is observed in the FT-IR spectra that exhibits a peak at 3000-2800 cm-1, denoting an amine salt.

Figure 3: Docked poses of imine compounds 2j, 2n, 2o docked against Yersinia pestis DHPS (PDB: 5JQ9). Based on docking results, these compounds exhibited a higher affinity to the enzyme compared to the endogenous ligand. A) Docked pose of 2j. B) Docked pose of 2n. C) Docked pose of 2o.

Table 2: Data on the amine compounds used in this study. Column 2 consists of diagrams of the R group substitution on the A ring for each amine compound. Column 3 shows the R2 groups for each amine compound. Column 4 shows TPSA (total polar surface area) values in angstroms. Column 5 displays the cLogP value for each amine compound determining its partition coefficient between n-octanol and water. Column 6 shows the drug scores of each amine compound. Column 7 shows the docking scores calculated in kcal/mol.
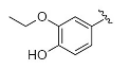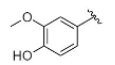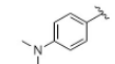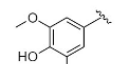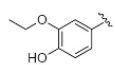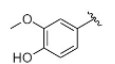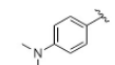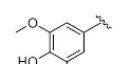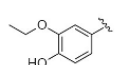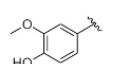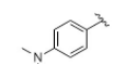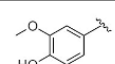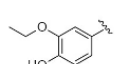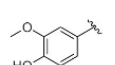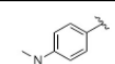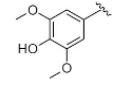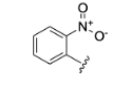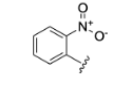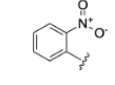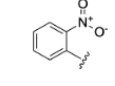
Compound	Ring A	R_2	TPSA	cLogP	Drug Score	Docking Score
3a		COOH	78.79 Å^2	2.20 nmoles/mg	0.49	-6.6 kcal/mol
3b		COOH	78.79 Å^2	1.79 nmoles/mg	0.79	-6.4 kcal/mol
3c		COOH	52.57 Å^2	2.11 nmoles/mg	0.38	-5.9 kcal/mol
3d		COOH	88.02 Å^2	1.72 nmoles/mg	0.81	-6.3 kcal/mol
3e		NO$_2$	87.31 Å^2	1.79 nmoles/mg	0.43	-6.3 kcal/mol
3f		NO$_2$	87.31 Å^2	1.39 nmoles/mg	0.44	-6.3 kcal/mol
3g		NO$_2$	61.09 Å^2	1.70 nmoles/mg	0.26	-5.7 kcal/mol
3h		NO$_2$	96.54 Å^2	1.32 nmoles/mg	0.44	-5.9 kcal/mol
3i		SO$_3$H	104.20 Å^2	0.49 nmoles/mg	0.19	-6.6 kcal/mol
3j		SO$_3$H	104.2 Å^2	0.08 nmoles/mg	0.28	-6.9 kcal/mol
3k		SO$_3$H	78.02 Å^2	0.39 nmoles/mg	0.15	-5.6 kcal/mol
3l		SO$_3$H	113.4 Å^2	0.01 nmoles/mg	0.3	-6.1 kcal/mol
3m		SO$_2$NH$_2$	110.0 Å^2	1.48 nmoles/mg	0.74	-6.7 kcal/mol
3n		SO$_2$NH$_2$	110.0 Å^2	1.07 nmoles/mg	0.89	-6.8 kcal/mol
3o		SO$_2$NH$_2$	83.81 Å^2	1.39 nmoles/mg	0.51	-5.6 kcal/mol

Table 2 continued

3p		SO_2NH_2	119.2 Å^2	1.00 nmoles/mg	0.88	-5.8 kcal/mol
3q		COOH	95.15 Å^2	1.29 nmoles/mg	0.44	-6.0 kcal/mol
3r		NO_2	103.6 Å^2	0.88 nmoles/mg	0.42	-5.9 kcal/mol
3s		SO_3H	120.6 Å^2	-0.43 nmoles/mg	0.17	-6.2 kcal/mol
3t		SO_2NH_2	126.3 Å^2	0.57 nmoles/mg	0.44	-5.8 kcal/mol

Docking

In this study, all 40 compounds were docked in *Yersinia pestis* DHPS, using AutoDock Vina. The results show that the free energy of binding for these biaryl imine and amine compounds was much greater than the binding energy of the endogenous ligand. Generally, the imine compounds exhibited greater binding affinity to DHPS in comparison to the amines. This could be a result of the entropic loss exhibited by amine compounds with a rotatable C-N bond, which becomes fixed upon binding. Molecules with a carboxyl group on the electron withdrawing side generally had greater free energy of binding, while on the other hand, molecules with a sulfonamide group on the electron withdrawing side had lower free energy of binding. This could be a result of the steric interference between the additional amine group on the sulfonamide and the side chains of DHPS. More aryl substitutions had better binding affinity out of the molecules that were tested.

Drug score

Compounds in this study were scanned via the Osiris property predictor, which determined a drug score based on various properties of the molecules such as cLogP, total polar surface area, molecular weight, and toxicity risk based on an existing library of drugs. Overall, the compounds in the study exhibited a relatively low drug score, which is a result of toxicity risk and total polar surface area. These calculations, along with Lipinski's rule of five, are assumptions derived upon preexisting drugs and as a result, a low drug score does not directly correlate with lower efficacy. However, a molecule that fits the description dictated by Lipinski's rule and the Osiris scanner generally have a higher chance of being effective.

Kirby Bauer

Upon testing these compounds through a Kirby Bauer assay at 1 mM concentration of the compound, it was shown that none of these compounds were effective at this concentration. The same procedure was repeated with 10 mM concentration of the compound and it was shown that around half of the compounds exhibited biological activity against the species: *N. sicca, B. cereus, E. coli,* and *S. epidermidis.* In this study, *N. sicca* was omitted because it exhibited negligible bacteria growth. Although some of these compounds present
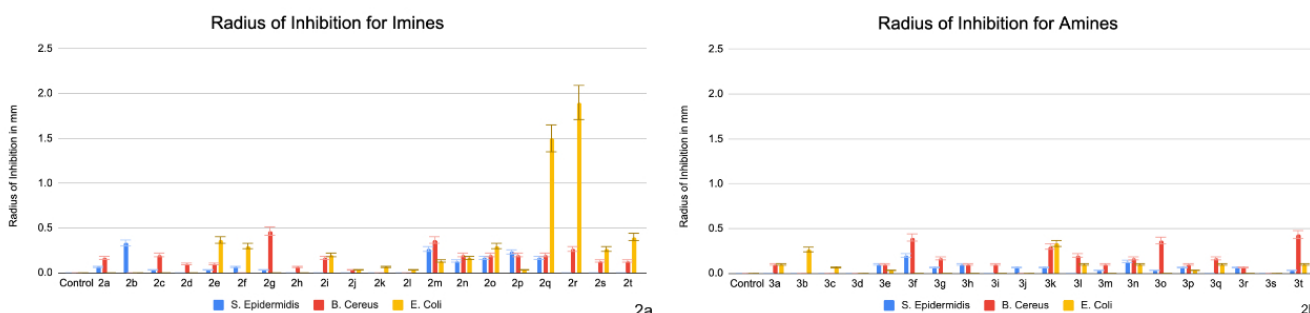
Figure 4: The radius of inhibition in millimeters for the imine and amine compounds on *S. epidermidis.* A) The radius of inhibition in millimeters for the imine compounds on *S. epidermidis, E. coli,* and *B. cereus.* The bars indicate average radius with an error bar with standard deviation. **B)** The radius of inhibition in millimeters for the amine compounds on *S. epidermidis, E. coli,* and *B. cereus.* The bars indicate average radius with an error bar with standard deviation.

biological activity at 10 mM, this is considered as an extremely concentrated solution and therefore these compounds are not viable therapeutic options. However, there are a few trends that are worth nothing among these 40 compounds. Overall, the amine compounds exhibited close to no biological activity. Imine compounds with sulfanilamide groups were favored and resulted in a higher radius of inhibition in comparison to the other groups. This is expected because sulfanilamide groups have been shown to inhibit various enzymes including DHPS. The sulfanilic acid group also resulted in a higher radius if inhibition in comparison to the other groups. The higher activity of these two groups could be due to the presence of more electron withdrawing atoms which allows for hydrogen bonding interactions between the protein and substrate. The data did not provide enough information to determine a trend between the three bacteria species.

Docking comparison

Overall, most of the results obtained from docking did not correlate with the actual biological activity of the compounds in this study. Although the compounds exhibited a high free energy of binding, they did not perform well *in vitro*, which demonstrates that binding is necessary but not sufficient for biological activity and inhibition. The docking results also predicted that the sulfanilamide group would exhibit worse binding, but the Kirby Bauer assay revealed that this functional group worked better than others. However, the docking results successfully predicted that imine compounds would perform better than amine compounds. Due to the structural similarity of imines and amines, there are no differences in the absorption and distribution of these molecules in bacterial cells. The only factor that determines the difference in activity between these two classes of molecules will be their ability to bind to the enzyme.

Overall Implications

The information received from conducting this study indicates that the pterin binding pocket of DHPS is a viable area of research that could potentially result in more effective antibiotics targeting it. The molecules developed in this study indicated that only a few were effective and required high concentrations to be viable in various assays such as the Kirby Bauer assay. A future study that could be developed would be based on finding the relationship between the docking scores of molecules and their biological effectiveness. One thing mentioned was that there was very little correlation between the docking score calculated and the biological efficacy of molecules from the radius of inhibition. This correlation could be studied more to determine what effects the biological efficacy of the molecules tested since it is not docking scores.

MATERIALS AND METHODS
Chemical synthesis
General procedure for imine condensation

In a glass round bottom flask equipped with a Teflon stir bar, (1 eq.) aryl aldehyde and catalytic phosphoric acid was added to a solution of 4-substituted aniline stirring in ethanol. The solution was heated to reflux for 0.5 hours, and the progress of the reaction was monitored by thin-layer chromatography (TLC). Upon the disappearance of the starting material and complete conversion to the product, the reaction was worked up and extracted with ethyl acetate over water. The resulting

organic layers were dried over anhydrous magnesium sulfate and concentrated *in vacuo*; the resulting material was purified by recrystallization from hot ethanol or isopropanol to give imine as a brightly colored solid in 82% to 98% yield.

General protocol for amine synthesis

In a glass round bottom flask equipped with a Teflon stir bar, solution of the imine was prepared in anhydrous isopropyl alcohol, to which 2 eq. of sodium borohydride was added. The reaction was stirred and mildly heated for 0.5 hours and was monitored by thin-layer chromatography (TLC) using a ninhydrin stain. After a complete reduction of the imine compound, the reaction was quenched and extracted with ethyl acetate over water. The organic layer was dried over anhydrous magnesium sulfate and concentrated *in vacuo*. The products were purified and recovered by recrystallization in ethanol or tetrahydrofuran (THF) to yield the amine product as a palely colored solid in 90% to 98% yield.

All solvents used were ACS grade, except solvents used for LC-MS, which were HPLC grade. Isopropanol was purchased from Stellar Chemical Corp., and tetrahydrofuran and ethyl acetate were purchased from J.T. Baker or Carolina Chemical. All other reagents for chemical synthesis were purchased from Sigma Aldrich, Acros Organics, Fluka Chemical, Alfa Aesar, HiMedia, or AK Scientific (> 95% purity) and were used without additional purification.

All compounds were characterized by Fourier-Transform Infrared (FT-IR) spectroscopy on a Thermo Nicolet iS5 FT-IR spectrometer with an iD5 attenuated total reflectance (ATR) assembly. They were also characterized by liquid chromatography-mass spectrometry (LC-MS) on a Thermo LTQ-XL linear ion trap mass spectrometer equipped with an electrospray ionization source (ESI) and with a Thermo Finnigan Surveyor high-performance liquid chromatography (HPLC) using a C8 reverse phase column. The full characterization of each compound is available in the supplementary materials.

In silico pharmacokinetic properties screening

Chemical properties, such as total polar surface area, molecular weight, and clogP, were determined by the OSIRIS property scanner and recorded as a single drug-likeness score (17).

In vitro testing

Cytotoxicity of all 40 compounds was tested on three different species of bacteria: *Escherichia coli, Staphylococcus epidermidis, and Bacillus cereus*. Bacterial species were purchased from Carolina Biological Supply, and overnight cultures were prepared in LB media. The bacteria were streaked on 10 cm Petri dishes in Mueller Hinton agar, and a Kirby Bauer assay was performed using solutions of the compounds at 10 mM and 1 mM loaded onto pre-sterilized paper discs, along with a negative control (10% DMSO without added compound). Radii of inhibition (ROI) were measured using digital calipers, and trials for all compounds were conducted in triplicate. Paper discs were briefly soaked in a solution of the compound, and bacteria were incubated for 24 hours before measuring radii of inhibition

Docking

All compounds were modeled through Avogadro, a

program used to build and visualize chemical structures (16). The appropriate protonation states were determined by assuming the pH of DHPS to be equal to bulk physiological pH at 7.4. An initial molecular mechanics geometry pre-optimization with a Universal Force Field (UFF) at 4 scans was applied to all molecules, while input files for quantum mechanical structural optimization were generated through Avogadro.

Density functional theory (DFT) optimizations, necessary for accurate prediction of thermodynamically minimized geometries of each compound, were completed using ORCA ver 4.2 (17), an *ab initio* program for quantum molecular modeling. Density functional theory (DFT) optimizations were completed with a B3LYP functional, def2-SVP basis set. Density functional theory calculations were performed on a Lenovo Thinkpad x1 8th Generation Intel® Core™ i5-8265U Processor (1.60 GHz).

All 40 compounds in this study were docked to the crystal structure of *Yersinia pestis* dihydropteroate synthase (PDB: 5JQ9) (15), via AutoDock Vina and AutoDock Tools, and free energies of binding were recorded. When co-optimized during docking, amino acid side chains on DHPS showed up to 5Å of flexibility from the ligand in the predicted binding mode. Predicted binding modes were ranked by the free energy of binding (ΔG) in kcal/mol. The resulting binding poses were visualized using PyMOL (18).

ACKNOWLEDGEMENTS

REFERENCES
1. "About Antibiotic Resistance." *Centers for Disease Control and Prevention*, Centers for Disease Control and Prevention, 13 Mar. 2020, www.cdc.gov/drugresistance/about.html.
2. "Be Antibiotics Aware: Smart Use, Best Care." *Centers for Disease Control and Prevention*, Centers for Disease Control and Prevention, 10 Mar. 2020, www.cdc.gov/patientsafety/features/be-antibiotics-aware.html.
3. Hammoudeh, Dalia I *et al.* "Replacing Sulfa Drugs with Novel DHPS Inhibitors." *Future Medicinal Chemistry* vol. 5,11 (2013): 1331-40. doi:10.4155/fmc.13.97
4. Yun, Mi-Kyung *et al.* "Catalysis and Sulfa Drug Resistance in Dihydropteroate Synthase." *Science* vol. 335,6072 (2012): 1110-4. doi:10.1126/science.1214641
5. A. Alsughayer, A. Elassar, S. Mustafa and F. Sagheer, "Synthesis, Structure Analysis and Antibacterial Activity of New Potent Sulfonamide Derivatives," *Journal of Biomaterials and Nanobiotechnology*, Vol. 2 No. 2, 2011, pp. 143-148. doi: 10.4236/jbnb.2011.22018.
6. Apaydın, Sinem, and Marianna Török. "Sulfonamide Derivatives as Multi-target Agents for Complex Diseases." *Bioorganic & Medicinal Chemistry Letters* vol. 29,16 (2019): 2042-2050. doi:10.1016/j.bmcl.2019.06.041
7. Cho, Min-Hyung, *et al.* "Structure-based Design and Biochemical Evaluation of Sulfanilamide Derivatives as Hepatitis B Virus Capsid Assembly Inhibitors." *Journal of Enzyme Inhibition and Medicinal Chemistry* 28.5 (2013): 916-925.
8. Hevener, Kirk E., *et al.* "Structural Studies of Pterin-based Inhibitors of Dihydropteroate Synthase." *Journal of Medicinal Chemistry* 53.1 (2010): 166-177.
9. Dennis, Matthew L., *et al.* "8-Mercaptoguanine Derivatives as Inhibitors of Dihydropteroate Synthase." *Chemistry-A European Journal* 24.8 (2018): 1922-1930.
10. Sun, Haoyu, *et al.* "A Deep Insight into the Toxic Mechanism for Sulfonamides Based on Bacterial Cell-cell Communication." *Environment International* 129 (2019): 185-193.
11. Neidle, Stephen. *Therapeutic Applications of Quadruplex Nucleic Acids*. Academic Press, 2012.
12. "E. Coli and Food Safety." *Centers for Disease Control and Prevention*, Centers for Disease Control and Prevention, 9 June 2020, www.cdc.gov/foodsafety/communication/ecoli-and-food-safety.html?CDC_AA_refVal=www.cdc.gov/features/ecoliinfection/index.html.
13. Blum, R. A., and K. A. Rodvold. "Recognition and Importance of Staphylococcus epidermidis Infections." *Clinical Pharmacy* 6.6 (1987): 464.
14. Bottone, Edward J. "Bacillus Cereus, a Volatile Human Pathogen." *Clinical Microbiology Reviews* 23.2 (2010): 382-398.
15. Zhao, Ying, *et al.* "Pterin–sulfa Conjugates as Dihydropteroate Synthase Inhibitors and Antibacterial Agents." *Bioorganic & Medicinal Chemistry Letters* 26.16 (2016): 3950-3954.
16. Hanwell, Marcus D., *et al.* "Avogadro: an Advanced Semantic Chemical Editor, Visualization, and Analysis Platform." *Journal of Cheminformatics* 4.1 (2012): 17.
17. Sander, Thomas. "OSIRIS Property Explorer." *Organic Chemistry Portal* (2001).
18. Neese, Frank. "Software update: the ORCA program system, version 4.2." *Wiley Interdisciplinary Reviews: Computational Molecular Science* 8.1 (2018): e1327.
19. Schrödinger, L. L. C. "The PyMOL Molecular Graphics System, Version 2.0 Schrödinger, LLC (2017)."
20. Morris, Garrett M., *et al.* "AutoDock4 and AutoDockTools4: Automated Docking with Selective Receptor Flexibility." *Journal of Computational Chemistry* 30.16 (2009): 2785-2791.

Supplemental Information of *"Rational design, combinatorial synthesis, and antimicrobial activity of novel biaryl imines and amines as potential competitive inhibitors of dihydropteroate synthase"*

Compound 2a [(E)-4-((3-ethoxy-4-hydroxybenzylidene)amino)benzoic acid]:
FTIR (ATR): v = 2950-2980 cm^{-1} (N-H / O-H bend), 1690-1710 cm^{-1} (C=N bend).
LCMS (ESI-MS): m/z calc'd for C$_{16}$H$_{15}$NO$_4^-$ [M - H$^+$]: 284.100109, found: 284.19.

Compound 2b [(E)-4-((4-hydroxy-3-methoxybenzylidene)amino)benzoic acid]:
FTIR (ATF): v = 2950-2980 cm^{-1} (N-H / O-H bend), 1680-1710 cm^{-1} (C=N bend).
LCMS (ESI-MS): m/z calc'd for C$_{15}$H$_{13}$NO$_4^-$ [M - H$^+$]: 270.084459, found: 270.12.

Compound 2c [(E)-4-((4-(dimethylamino)benzylidene)amino)benzoic acid]:
FTIR (ATR): *v* = 2950-2980 cm^{-1} (N-H bend), 1690-1700 cm^{-1} (C=N bend).
LCMS (ESI-MS): m/z calc'd for C$_{16}$H$_{16}$N$_2$O$_3^-$ [M - H$^+$]: 283.116093, found: 283.14.

Compound 2d [(E)-4-((4-hydroxy-3,5-dimethoxybenzylidine)amino)benzoic acid]:
FTIR (ATF): v = 2950-2980 cm^{-1} (N-H / O-H bend), 1690-1710 cm^{-1} (C=N bend).
LCMS (ESI-MS): m/z calc'd for C$_{16}$H$_{15}$NO$_5^-$ [M + H$^+$]: 302.095023, found: 302.12.

Compound 2e [(E)-2-ethoxy-4-(((4-nitrophenyl)imino)methyl)phenol]:
FTIR (ATF): v = 2950-2980 cm^{-1} (N-H / O-H bend), 1690-1700 cm^{-1} (C=N bend).
LCMS (ESI-MS): m/z calc'd for C$_{15}$H$_{14}$N$_2$O$_4^+$ [M - H$^+$]: 285.095358, found: 285.59.

Compound 2f [(E)-2-methoxy-4-(((4-nitrophenyl)imino)methyl)phenol]:
FTIR (ATF): v = 2950-2980 cm^{-1} (N-H / O-H bend), 1680-1710 cm^{-1} (C=N bend).
LCMS (ESI-MS): m/z calc'd for C$_{13}$H$_{12}$N$_2$O$_4^+$ [M + H$^+$]: 261.079708, found: 261.31.

Compound 2g [(E)-N,N-dimethyl-4-(((4-nitrophenyl)imino)methyl)aniline]:
FTIR (ATF): v = 2950-2980 cm^{-1} (N-H / O-H bend), 1690-1710 cm^{-1} (C=N bend).
LCMS (ESI-MS): m/z calc'd for C$_{15}$H$_{15}$N$_3$O$_2^+$ [M - H$^+$]: 268.116427, found: 268.29.

Compound 2h [(E)-2,6-dimethoxy-4-(((4-nitrophenyl)imino)methyl)phenol]:
FTIR (ATF): v = 2950-2980 cm^{-1} (N-H / O-H bend), 1670 cm^{-1} (C=N bend).
LCMS (ESI-MS): m/z calc'd for C$_{15}$H$_{14}$N$_2$O$_5^+$ [M - H$^+$]: 301.090273, found: 301.02.

Compound 2i [(E)-4-((3-ethoxy-4-hydroxybenzylidene)amino)benzenesulfonic acid]:
FTIR (ATF): v = 2950-2980 cm^{-1} (N-H / O-H bend), 1680 cm^{-1} (C=N bend).
LCMS (ESI-MS): m/z calc'd for $C_{15}H_{15}NO_5S^+$ [M + H$^+$]: 322.067096, found: 322.06.

Compound 2j [(E)-4-((4-hydroxy-3-methoxybenzylidene)amino)benzenesulfonic acid]:
FTIR (ATF): v = 2950-2980 cm^{-1} (N-H / O-H bend), 1690-1700 cm^{-1} (C=N bend).
LCMS (ESI-MS): m/z calc'd for $C_{14}H_{13}NO_5S^+$ [M + H$^+$]: 308.051446, found: 308.004.

Compound 2k [(E)-4-((4-(dimethylamino)benzylidene)amino)benzenesulfonic acid]:
FTIR (ATF): v = 2950-2980 cm^{-1} (N-H / O-H bend), 1690 cm^{-1} (C=N bend).
LCMS (ESI-MS): m/z calc'd for $C_{15}H_{16}N_2O_3S^+$ [M - H$^+$]: 303.088165, found: 303.03.

Compound 2l [(E)-4-((4-hydroxy-3,5-dimethoxybenzylidene)amino)benzenesulfonic acid]:
FTIR (ATF): v = 2950-2980 cm^{-1} (N-H / O-H bend), 1680 cm^{-1} (C=N bend).
LCMS (ESI-MS): m/z calc'd for $C_{15}H_{15}NO_6S^+$ [M - H$^+$]: 336.062011, found: 336.31.

Compound 2m [(E)-4-((3-ethoxy-4-hydroxybenzylidene)amino)benzenesulfonamide]:
FTIR (ATF): v = 2950-2980 cm^{-1} (N-H / O-H bend), 1660 cm^{-1} (C=N bend).
LCMS (ESI-MS): m/z calc'd for $C_{15}H_{16}N_2O_4S^+$ [M - H$^+$]: 319.083080, found: 319.46.

Compound 2n [(E)-4-((4-hydroxy-3-methoxybenzylidene)amino)benzenesulfonamide]:
FTIR (ATF): v = 2950-2980 cm^{-1} (N-H / O-H bend), 1670 cm^{-1} (C=N bend).
LCMS (ESI-MS): m/z calc'd for $C_{14}H_{14}N_2O_4S^+$ [M - H$^+$]: 305.067430, found: 305.07.

Compound 2o [(E)-4-((4-(dimethylamino)benzylidene)amino)benzenesulfonamide]:
FTIR (ATF): v = 2950-2980 cm^{-1} (N-H / O-H bend), 1690 cm^{-1} (C=N bend).
LCMS (ESI-MS): m/z calc'd for $C_{15}H_{17}N_3O_2S^+$ [M - H$^+$]: 302.104149, found: 302.18.

Compound 2p [(E)-4-((4-hydroxy-3,5-dimethyoxybenzylidene)amino)benzenesulfonamide]:
FTIR (ATF): v = 2950-2980 cm^{-1} (N-H / O-H bend), 1680- 1690 cm^{-1} (C=N bend).
LCMS (ESI-MS): m/z calc'd for $C_{15}H_{16}N_2O_5S^+$ [M - H$^+$]: 335.077995, found: 335.29.

Compound 2q [(E)-4-((2-nitrobenzylidene)amino)benzoic acid]:
FTIR (ATF): v = 2950-2980 cm^{-1} (N-H / O-H bend), 1690 cm^{-1} (C=N bend).
LCMS (ESI-MS): m/z calc'd for $C_{14}H_{10}N_2O_4^+$ [M + H$^+$]: 271.064058, found: 271.08.

Compound 2r [(E)-1-(2-nitrophenyl)-N-(4-nitrophenyl)methanimine]:
FTIR (ATF): v = 2950-2980 cm^{-1} (N-H / O-H bend), 1690 cm^{-1} (C=N bend).
LCMS (ESI-MS): m/z calc'd for $C_{13}H_9N_3O_4^+$ [M - H$^+$]: 270.059307, found: 270.48.

Compound 2s [(E)-4-((2-nitrobenzylidene)amino)benzenesulfonic acid]:
FTIR (ATF): ν = 2950-2980 cm^{-1} (N-H / O-H bend), 1690-1710 cm^{-1} (C=N bend).
LCMS (ESI-MS): m/z calc'd for C$_{13}$H$_{10}$N$_2$O$_5$S$^+$ [M + H$^+$]: 307.031045, found: 307.36.

Compound 2t [(E)-4-((2-nitrobenzylidene)amino)benzenesulfonamide]:
FTIR (ATF): ν = 2950-2980 cm^{-1} (N-H / O-H bend), 1690-1700 cm^{-1} (C=N bend).
LCMS (ESI-MS): m/z calc'd for C$_{13}$H$_{11}$N$_3$O$_4$S$^+$ [M - H$^+$]: 304.047029, found: 304.04.

Compound 3a [4-((3-ethoxy-4-hydroxybenzyl)amino)benzoic acid]:
FTIR (ATF): ν = 2950-2980 cm^{-1} (N-H / O-H bend), 1250-1300 cm^{-1} (C-N bend).
LCMS (ESI-MS): m/z calc'd for C$_{16}$H$_{16}$NO$_4$$^+$ [M + H$^+$]: 287.107934, found: 287.45.

Compound 3b [4-((4-hydroxy-3-methoxybenzyl)amino)benzoic acid]:
FTIR (ATF): ν = 2950-2980 cm^{-1} (N-H / O-H bend), 1250-1300 cm^{-1} (C-N bend).
LCMS (ESI-MS): m/z calc'd for C$_{15}$H$_{14}$NO$_4$$^+$ [M - H$^+$]: 271.092284, found: 271.02.

Compound 3c [4-((4-(dimethylamino)benzyl)amino)benzoic acid]:
FTIR (ATF): ν = 2950-2980 cm^{-1} (N-H / O-H bend), 1250-1300 cm^{-1} (C-N bend).
LCMS (ESI-MS): m/z calc'd for C$_{18}$H$_{17}$N$_2$O$_3$$^+$ [M + H$^+$]: 310.123918, found: 310.27.

Compound 3d [4-((4-hydroxy-3,5-dimethoxybenzyl)amino)benzoic acid]:
FTIR (ATF): ν = 2950-2980 cm^{-1} (N-H / O-H bend), 1250-1280 cm^{-1} (C-N bend).
LCMS (ESI-MS): m/z calc'd for C$_{16}$H$_{16}$NO$_5$$^+$ [M + H$^+$]: 303.102849, found: 303.12.

Compound 3e [2-ethoxy-4-(((4-nitrophenyl)amino)methyl)phenol]:
FTIR (ATF): ν = 2950-2980 cm^{-1} (N-H / O-H bend), 1250-1280 cm^{-1} (C-N bend).
LCMS (ESI-MS): m/z calc'd for C$_{15}$H$_{15}$N$_2$O$_4$$^+$ [M - H$^+$]: 288.103183, found: 288.39.

Compound 3f [2-methoxy-4-(((4-nitrophenyl)amino)methyl)phenol]:
FTIR (ATF): ν = 2950-2980 cm^{-1} (N-H / O-H bend), 1250-1300 cm^{-1} (C-N bend).
LCMS (ESI-MS): m/z calc'd for C$_{14}$H$_{13}$N$_2$O$_4$$^+$ [M - H$^+$]: 272.087533, found: 272.09.

Compound 3g [N,N-dimethyl-4-(((4-nitrophenyl)amino)methyl)aniline]:
FTIR (ATF): ν = 2950-2980 cm^{-1} (N-H / O-H bend), 1280-1300 cm^{-1} (C-N bend).
LCMS (ESI-MS): m/z calc'd for C$_{15}$H$_{16}$N$_3$O$_2$$^+$ [M + H$^+$]: 271.124252, found: 271.18.

Compound 3h [2,6-dimethoxy-4-(((4-nitrophenyl)amino)methyl)phenol]:
FTIR (ATF): ν = 2950-2980 cm^{-1} (N-H / O-H bend), 1250-1280 cm^{-1} (C-N bend).
LCMS (ESI-MS): m/z calc'd for C$_{15}$H$_{15}$N$_2$O$_5$$^+$ [M - H$^+$]: 302.098098, found: 302.23.

Compound 3i [4-((3-ethoxy-4-hydroxybenzyl)amino)benzenesulfonic acid]:
FTIR (ATF): ν = 2950-2980 cm^{-1} (N-H / O-H bend), 1250-1280 cm^{-1} (C-N bend).

LCMS (ESI-MS): m/z calc'd for $C_{15}H_{16}NO_5S^+$ [M - H$^+$]: 321.074921, found: 321.04.

Compound 3j [4-((4-hydroxy-3-methoxybenzyl)amino)benzenesulfonic acid]:
FTIR (ATF): v = 2950-2980 cm^{-1} (N-H / O-H bend), 1250-1280 cm^{-1} (C-N bend).
LCMS (ESI-MS): m/z calc'd for $C_{14}H_{14}NO_5S^+$ [M - H$^+$]: 307.059270, found: 307.24.

Compound 3k [4-((4-(dimethylamino)benzyl)amino)benzenesulfonic acid]:
FTIR (ATF): v = 2950-2980 cm^{-1} (N-H / O-H bend), 1250-1300 cm^{-1} (C-N bend).
LCMS (ESI-MS): m/z calc'd for $C_{15}H_{17}N_2O_3S^+$ [M + H$^+$]: 306.095990, found: 306.15.

Compound 3l [4-((4-hydroxy-3,5-dimethoxybenzyl)amino)benzenesulfonic acid]:
FTIR (ATF): v = 2950-2980 cm^{-1} (N-H / O-H bend), 1250-1280 cm^{-1} (C-N bend).
LCMS (ESI-MS): m/z calc'd for $C_{15}H_{16}NO_6S^+$ [M + H$^+$]: 339.069836, found: 339.01.

Compound 3m [4-((3-ethoxy-4-hydroxybenzyl)amino)benzenesulfonamide]:
FTIR (ATF): v = 2950-2980 cm^{-1} (N-H / O-H bend), 1250-1280 cm^{-1} (C-N bend).
LCMS (ESI-MS): m/z calc'd for $C_{15}H_{17}N_2O_4S^+$ [M + H$^+$]: 322.090905, found: 322.00.

Compound 3n [4-((4-hydroxy-3-methoxybenzyl)amino)benzenesulfonamide]:
FTIR (ATF): v = 2950-2980 cm^{-1} (N-H / O-H bend), 1250-1280 cm^{-1} (C-N bend).
LCMS (ESI-MS): m/z calc'd for $C_{14}H_{15}N_2O_4S^+$ [M + H$^+$]: 308.075254, found: 308.04.

Compound 3o [4-((4-(dimethylamino)benzyl)amino)benzenesulfonamide]:
FTIR (ATF): v = 2950-2980 cm^{-1} (N-H / O-H bend), 1250-1300 cm^{-1} (C-N bend).
LCMS (ESI-MS): m/z calc'd for $C_{15}H_{18}N_3O_2S^+$ [M + H$^+$]: 305.111974, found: 305.08.

Compound 3p [4-((4-hydroxy-3,5-dimethoxybenzyl)amino)benzenesulfonamide]:
FTIR (ATF): v = 2950-2980 cm^{-1} (N-H / O-H bend), 1250-1280 cm^{-1} (C-N bend).
LCMS (ESI-MS): m/z calc'd for $C_{15}H_{17}N_2O_5S^+$ [M - H$^+$]: 336.085820, found: 336.16.

Compound 3q [4-((2-nitrobenzyl)amino)benzoic acid]:
FTIR: (ATR) v = 2950-2980 cm^{-1} (N-H / O-H bend), 1570 cm^{-1} (N-H bend), 1250-1270 cm^{-1} (C-N bend).
LCMS (ESI-MS): m/z calc'd for $C_{14}H_{11}N_2O_4^+$ [M - H$^+$]: 270.071883, found: 270.06.

Compound 3r [4-nitro-N-(2-nitrobenzyl)aniline]:
FTIR: (ATR): v = 2950-2980 cm^{-1} (N-H / O-H bend), 1550 cm^{-1} (N-H bend), 1250-1270 cm^{-1} (C-N bend).
LCMS (ESI-MS): m/z calc'd for $C_{13}H_{10}N_3O_4^+$ [M + H$^+$]: 273.067132, found: 273.03.

Compound 3s [4-((2-nitrobenzyl)amino)benzenesulfonic acid]:

FTIR: (ATR) v = 2950-2980 cm^{-1} (N-H / O-H bend), 1580 cm^{-1} (N-H bend), 1250-1300 cm^{-1} (C-N bend).

LCMS (ESI-MS): m/z calc'd for C$_{13}$H$_{11}$N$_2$O$_5$S$^+$ [M - H$^+$]: 306.038870, found: 306.02

Compound 3t [4-((2-nitrobenzyl)amino)benzenesulfonamide]:

FTIR (ATR): v = 2950-2980 cm^{-1} (N-H / O-H bend), 1560 cm^{-1}: (N-H bend), 1250-1270 cm^{-1}: (C-N bend).

LCMS (ESI-MS): m/z calc'd for C$_{13}$H$_{12}$N$_3$O$_4$S$^+$ [M + H$^+$]: 307.054854, found: 307.01.